ELSEVIER

Journal of Fluids and Structures 19 (2004) 851–862

JOURNAL OF FLUIDS AND STRUCTURES

www.elsevier.nl/locate/jnlabr/yjfls

Self-excited jet-precession Strouhal number and its influence on downstream mixing field

J. Mi*, G.J. Nathan

School of Mechanical Engineering, University of Adelaide, SA 5005, Australia

Received 19 July 2003; accepted 15 April 2004

Abstract

Luxton et al. (1987) discovered naturally occurring precession of a nonswirling, axisymmetric jet discharging into a large cylindrical chamber. The fluid-mechanical (fluidic) nozzle which generates this precessing jet (PJ) flow has found applications in industrial burners, providing stable flames, reduced pollutant emissions, and fuel savings. The low-frequency precession phenomenon is the key to achieve those benefits. However, its complexity is such that a detailed understanding of it is still in its infancy. The present study investigates the jet precession from a fluidic nozzle with a configuration similar to that of Luxton et al. It firstly assesses the variation in the precession frequency with the chamber length and jet velocity and then seeks to extend previous definitions of the precession Strouhal number for the flow emerging from the chamber outlet. Previous definitions are based on the characteristic velocity and length scales of the flow at the chamber inlet. The effects of both Strouhal and Reynolds numbers on the downstream mixing field are examined by measuring the total pressure variation along the nozzle axis at different values of these numbers. The influence of the Strouhal number is also explored by visualizing the PJ flames. It is demonstrated that the jet precession frequency increases approximately linearly as either the nozzle chamber length or the jet velocity increases, for the present range of conditions in which the precession occurs continuously. Also, the precession Strouhal number is found to have far stronger influence on the downstream mixing field than does the Reynolds number.

1. Introduction

Jet precession is a rotational oscillatory motion of the entire jet with respect to an axis other than the jet's own centreline. Luxton et al. (1987) discovered the naturally occurring, or self-excited, precession of an initially axisymmetric jet generated by a fluidic nozzle characterized by an orifice inlet, a large constant area chamber and an orifice outlet (see Fig. 1). After entering the chamber via the inlet, the jet expands through entrainment of chamber fluid and reattaches asymmetrically to the chamber wall. A strong vortex loop is generated when the reattached jet interacts with the exit orifice and this causes the jet to deflect sharply across the outlet cross-section. The asymmetric entrainment also feeds back to reinforce an azimuthal pressure difference which causes the reattachment point of the primary jet to move azimuthally around the inner surface of the chamber. The deflecting jet which leaves the chamber thus precesses about the nozzle axis. Simultaneously, external fluid is drawn into the chamber to replenish what is entrained by the primary jet. This fluid merges with a part of primary jet fluid which is re-circulated within the chamber and moves upstream with a strong swirl of the opposite sense to the precession. It is important to note that to produce the jet

*Corresponding author. Tel.: +61-8-8303-5170; fax: +61-8-8303-4367.
E-mail address: jcmi@mecheng.adelaide.edu.au (J. Mi).

0889-9746/$ - see front matter © 2004 Elsevier Ltd. All rights reserved.
doi:10.1016/j.jfluidstructs.2004.04.006

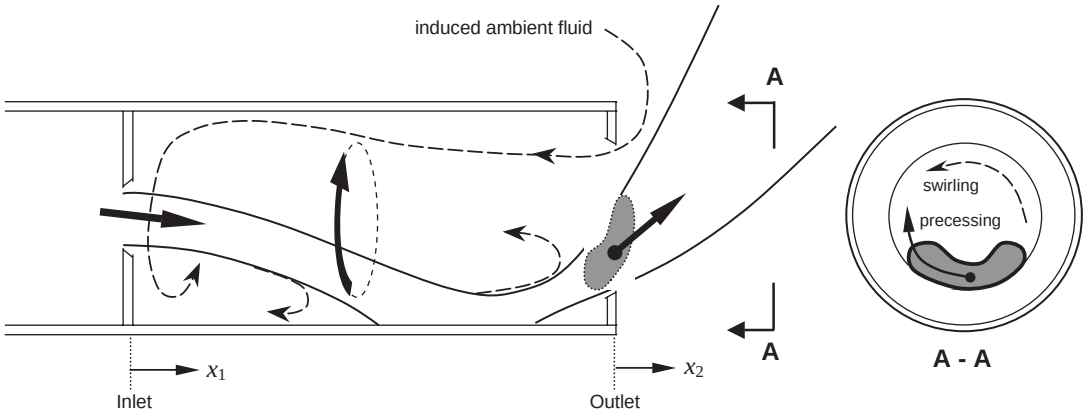

Fig. 1. Sketch of a precessing jet flow through a fluidic nozzle.

precession the nozzle configuration must be conditioned with the inlet expansion ratio, chamber length-to-diameter ratio and some other parameters [Luxton et al. (1987); Nathan (1988)].

The above fluidic precessing jet (FPJ) flow has found application in industrial burners (Manias and Nathan 1993, 1994; Manias et al. 1995). Full-scale installations of commercial gas-firing FPJ burner systems in rotary kilns in process industries (e.g. cement, lime and alumina) have consistently demonstrated that the FPJ flames deliver a reduction of typically 50% of NO_x emissions and, simultaneously, a fuel saving of about 5%, relative to those flames from the replaced burners (Manias and Nathan (1993, 1994); Manias et al. (1995)). It follows that the PJ burner technology has been under large-scale development through a collaborative research and development (R&D) program between the University of Adelaide and FCT Combustion Pty Limited. The ongoing program includes work on the flow inside the chamber which generates the precession [e.g., Hill et al. (1995); Nathan et al. (1998); Mi et al. (1999); Mi and Nathan (2000)] and outside the chamber in the region where combustion occurs [e.g., Nathan and Luxton (1991); Newbold et al. (2000)].

We have also conducted a study of the effects of precession on mixing characteristics of a round jet whose precession is generated by a mechanically rotating nozzle, Fig. 2, under controlled conditions (Schneider 1996; Nobes 1997; Mi et al. 1997, 1998; Mi and Nathan, 2004). The scientific advantage of the use of the mechanically precessing jet (MPJ) is that it has well-defined initial conditions, each of which can be varied independently. However, the requirement for moving components means that it is not practical for the harsh environments of furnaces and kilns. A key finding of the work for the MPJ is that the exit Strouhal number of precession, $St_e = f_p d_e / U_e$ (where f_p is the precessing frequency; d_e and U_e are, respectively, the jet diameter and bulk velocity at the nozzle exit), and the jet exit deflection angle (α) are two controlling parameters of the downstream flow development [Schneider (1996); Nobes (1997)]. However, only the effect of the Strouhal number has been examined profoundly because for the FPJ case the geometric ratios of the nozzle, such as the chamber length/diameter, have very trivial influence on the mean deflection angle ($\sim 60^\circ$) of the emerging jet (Nathan 1988; Mi 1996). In the case of $\alpha = 45^\circ$, features of the MPJ flow in the high-St_e regime, i.e., when $St_e \geqslant St_{cr}$ (the critical value), are significantly different from those for $St_e < St_{cr}$. These differences result in dramatic differences between the corresponding flames. For example, Nathan et al. (1996) found that MPJ flames for $St_e > St_{cr}$, are highly luminous and exhibit low strain, while those below it, $St_e < St_{cr}$, are highly strained and blue. Based on these observations, it is anticipated that the precession Strouhal number should also be a controlling parameter for turbulent mixing characteristics of the FPJ flow.

Direct translation of the findings from the MPJ nozzle to the FPJ nozzle is, however, not straightforward. There is growing evidence that there are significant differences between the two flows. An example is that the MPJ flow generates a central recirculation zone in the near field (Schneider et al. 1997a; Mi and Nathan, 2004) while the FPJ does not [Wong et al. (2003)]. Moreover, the emerging jet from the FPJ nozzle, Fig. 1, is not circular, but crescent shaped, in cross section [Wong et al. (2003)]. The fact that there has been no proper definition of the precession Strouhal number to characterize the FPJ flow downstream of the chamber outlet further complicate comparisons between the two flows. Instead, the existing definitions of Strouhal number [e.g., Hill et al. (1995); Nathan et al. (1998)] are based only on the flow conditions at the chamber *inlet* and so probably only truly characterize the precessing flow inside the chamber. To characterize the external downstream flow, it is necessary for the Strouhal number to use parameters based on local flow conditions at the chamber *outlet*. As we will demonstrate later in Section 3, the precession frequency of the FPJ is in fact

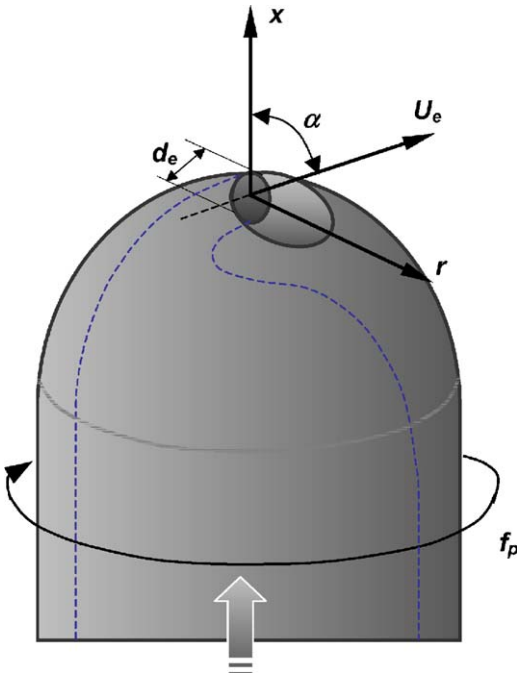

Fig. 2. Sketch of a mechanically rotating nozzle with relevant notations and definitions.

a strong function of the chamber length and so is the velocity profile at the chamber outlet (Wong et al. 2003). It is also important to note that there has been a lack of knowledge about how to extrapolate experimental results from the laboratory FPJ nozzle/burner to industrial applications which use much larger FPJ nozzles. The above issues motivate the present work with two specific aims. The first aim is to develop proper definitions of the Reynolds and precession Strouhal numbers to effectively characterize the downstream flow outside the chamber while the other is to determine which number is more influential to the mixing field. We believe that the present work will enhance our predictability on features of the industrial FPJ nozzles/burners via their laboratory tests.

The present paper first reports on the influence of chamber length and inlet Reynolds number (Re_1) on the frequency (f_p) of jet precession. It then defines the Reynolds number (Re_2) and precession Strouhal number (St_2) by relating the local velocity and length scales at the chamber outlet to those at the chamber inlet. Effects of the inlet velocity and chamber length on the new Reynolds and precession Strouhal numbers are checked using experimental data. Next, the impacts of Re_2 and St_2 on the downstream mixing field are investigated by measuring the downstream pressure fields at different values of Re_2 and St_2. Finally, we also explore the effect of the Strouhal number on the FPJ flames.

2. Experimental details

The experimental facility includes a plenum chamber to which various nozzles can be attached. The plenum is supplied with filtered and compressed air at pressures of up to 500 kPa at room temperature of approximately 20°C. The jet inlet velocity (U_1) for the present study were varied by changing the plenum pressure. The magnitude of U_1 was determined by the orifice-type flow meter with uncertainty of $\pm 1\%$. The configuration of the PJ nozzle is shown in Fig. 3. In the figure, d_1 represents the inlet diameter, D the chamber diameter, L the chamber length, L_c the distance between the inlet exit and the centre-body, d_c the centre-body diameter, s_c the distance between the centre-body and the chamber outlet exit, and d_2 the chamber outlet diameter. Three different-sized PJ nozzles of the same general configuration ($d_1/D \approx 0.19$) were used for the study; their chamber diameters are 13.4, 26.6 and 47.5 mm, respectively. The dimensions d_1, L, L_c and the Reynolds number $Re_1 \equiv U_1 d_1/\nu$, where U_1 is the inlet bulk mean velocity and ν is the kinematic viscosity, can be varied (within limit) in each nozzle.

The precession frequency f_p was measured using a hot-wire probe positioned downstream from and near to the chamber exit. The exact probe location for each nozzle was optimized to obtain a signal spectral density function with a

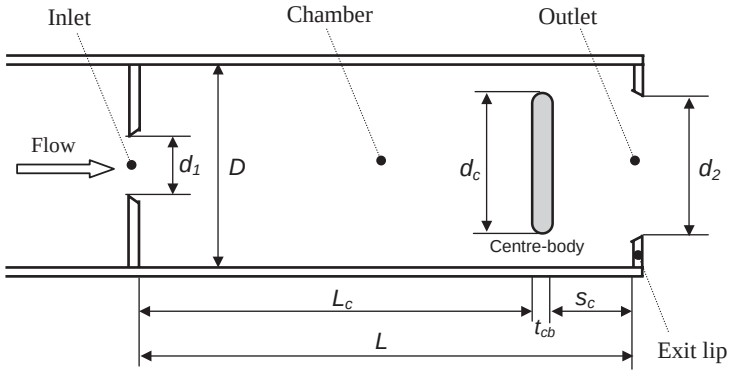

Fig. 3. Sketch of a fluidic precessing jet (FPJ) nozzle with relevant notations and definitions.

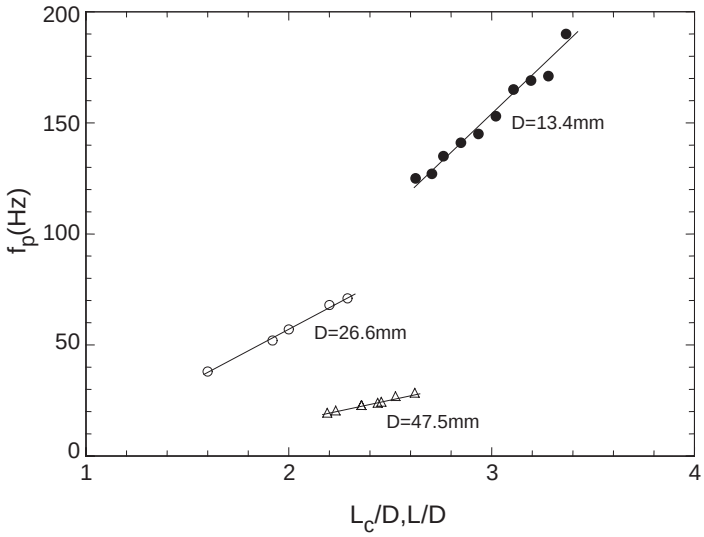

Fig. 4. Dependence of the precession frequency f_p on the chamber length L or L_c: ●, $D=13.4$ mm, $d_1/D\approx0.19$, $d_2/D\approx0.86$ and $Re_1\approx25{,}000$; △, 47.5 mm, 0.194, 1 and 65,000; ○, 26.6 mm, 0.19, 0.82 and 75,000.

distinct peak at the particular frequency of the precession. The hot wire was made of tungsten wire of 5 μm diameter and 1 mm length. The wire was operated by in-house constant temperature circuit with an overheat ratio of 1.5. The signal from the circuit was offset, amplified and then taken by a spectrum analyzer (HP3582A) for about a minute. The power spectra of the hot-wire signals were thus generated. A particular frequency of the jet precession for each nozzle configuration at a particular value of Re_1 was estimated from the corresponding spectrum. For some cases, the hot-wire signals were digitized using a 12-bit A/D converter (PC30) on a personal computer.

To check the effect of both the precession Strouhal and Reynolds numbers on the PJ flow outside the nozzle, total pressure measurements were made in the near field downstream and along the axis of the 26.6 mm nozzle. A single total pressure tube (i.d. = 0.2 mm) was used with an in-house pressure transducer. We also tested open flames from the 13.4 mm (brass) nozzle aligned vertically at different nozzle lengths. Instantaneous images of the flame were taken using a digital camera (Sony MVC-FD73).

3. Effects of chamber length and jet initial velocity on precession frequency

Fig. 4 shows the dependence of the precession frequency f_p on L_c/D (with a centre-body) and L/D (without centre-body). Experimental conditions for the measurements are provided in the figure caption. It is evident that f_p increases

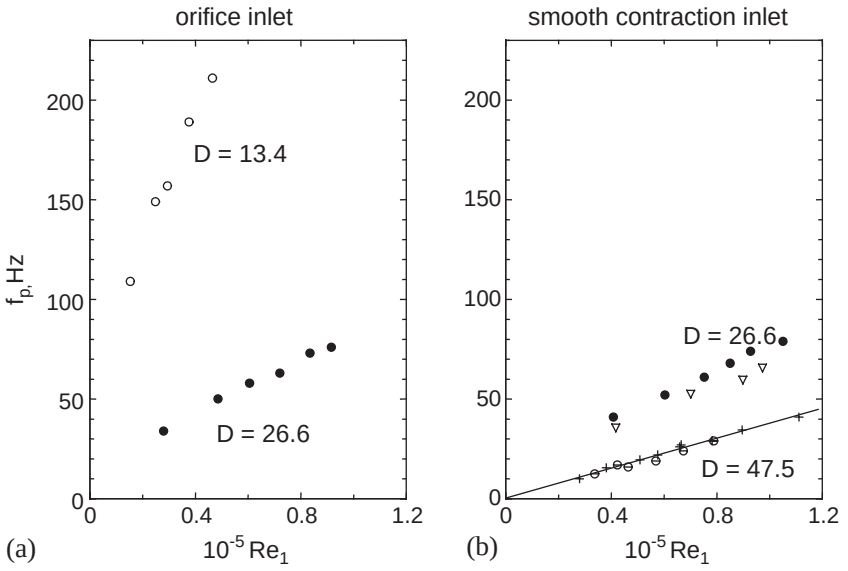

Fig. 5. Effect of the Reynolds number Re_1 on the precession frequency f_p. (a) Orifice-type inlet ($L_c/D = 2.2$): ●, $D = 13.4$ mm; $\mu = 26.6$ mm. (b) Smooth contraction inlet: ● ($L_c/D = 2.2$), 26.6 mm and with small inlet lip (0.2 mm); ▽ ($L_c/D = 2.2$), 26.6 mm and no inlet-lip; ⊖ ($L/D = 2.32$); + ($L/D = 2.49$), 47.5 mm and no lips.

approximately linearly as L or L_c increases over a certain range of the length where the precession occurs continuously. This feature applies to all the PJ nozzles tested here as shown in Fig. 4 and elsewhere [e.g., Mi et al. (1999)] so that it is generic. We can explain it as follows. The magnitude of f_p depends upon both the axial momentum of the jet, M_x, and the angular momentum of the swirling fluid (around the main jet), M_θ, at the upstream end of the chamber (see Fig. 1). If the ratio M_θ/M_x is greater, f_p will certainly increase. It can be argued that M_θ/M_x increases when lengthening the chamber. As indicated in Fig. 1, the swirling fluid is partly recirculated from the main jet itself and partly induced from the chamber outside (ambient fluid). As L increases, more swirling fluid will arise from the main jet (and less from the outside) and therefore more initially axial momentum will be converted to the angular momentum. As a result, the ratio M_θ/M_x (and hence f_p) increases.

Fig. 5 shows the dependence of f_p on $Re_1 (\equiv U_1 d_1/\nu)$ for each nozzle. The experimental conditions are given in the figure caption. (The frequency data were originally presented against the bulk velocity U_1. However, the range of U_1 for each nozzle is so different that the data sets for all the nozzles cannot be well put together on a single plot like Fig. 5.) For each PJ nozzle, f_p increases with Re_1 (or U_1), which is expected. As viewed from the six data sets, this variation appears linear and may be approximated by $f_p = C_0 + C_1 Re_1$, where C_0 and C_1 are experimental constants. It can be deduced from Fig. 5 that these constants depend fairly strongly on the jet inlet geometric configuration and, especially, the chamber diameter (D). That is, they are different from nozzle to nozzle. Interestingly, for the 47.5 mm nozzle with a smooth contraction inlet and no centre-body and no outlet lip (sudden contraction), extrapolation of the best-fit line of the data points converges closely to the origin of the coordinates, i.e., $C_0 \approx 0$. However, this is not generic; in fact, is $C_\phi \neq_\phi$ zero for the other configurations.

4. Previous definitions of precession Strouhal number with experimental data

Nathan and Luxton (1991) defined the Strouhal number of jet precession based on the conditions at the chamber inlet. They chose the height of the expansion step, $h = (D - d_1)/2$, and the jet bulk velocity at the inlet throat, U_1, for configurations with a narrow range of chamber lengths, i.e.

$$St_h \equiv \frac{f_p h}{U_1} = \frac{f_p \frac{1}{2}(D - d_1)}{U_1}. \quad (1)$$

If we define the conventional Strouhal number of the jet precession specifically for the flow confined in the chamber as

$$\mathrm{St}_1 \equiv \frac{f_p d_1}{U_1}, \tag{2}$$

then Eq. (1) can be rewritten as

$$\mathrm{St}_h = \frac{1}{2}\left(\frac{D}{d_1} - 1\right)\mathrm{St}_1. \tag{3}$$

Transposing the f_p data from Fig. 5, we obtained six data sets for the above-defined Strouhal number St_1 versus the Reynolds number Re_1 (Fig. 6). For the 47.5 mm nozzle at $L/D = 2.32$ and 2.49 and with no centre-body and no outlet-lip, the value of St_1 (≈ 0.0021) appears to be nearly independent of Re_1. By comparison, St_1 decreases slightly as Re_1 increases for the other two nozzles with a centre-body and the outlet-lip.

Definitions (1) and (2) were derived for a nozzle with fixed chamber length. They clearly do not account for the strong dependence of f_p on L or L_c (Fig. 4). Accordingly, St_1 must also be a function of L or L_c. This is demonstrated in Fig. 7 (right axis) which plots St_1 against f_p. Not only is the dependence approximately linear, but the data from the different nozzles appear to fit well along a single line.

Hill et al. (1995) observed a large scattering of the values of the precession Strouhal number based on the length scale $l_o = (D - d_1)/2$ [i.e., definition (1)], $l_o = d_1$ and $l_o = D$ for several different FPJ water flows fully confined within long ducts, with different sudden expansion ratios. Their observation led them to seek some alternative length scale for the Strouhal number. They used the initial momentum M of jet as the basis for the scaling of f_p, defining

$$\mathrm{St}_M \equiv \frac{f_p\sqrt{\rho}D^2}{\sqrt{M}}, \tag{4}$$

where ρ is the density of fluid. These authors found that definition (4) provides a good collapse of the data for those sudden expansions into a long duct. In their flows the frequency cannot be related to the chamber length because it is so long that it can be considered 'infinite'. Unlike the present configurations, in which the length-scale of the oscillating jet within the chamber evidently "locks on" to the chamber length, the oscillation in the long pipe will find its own "natural" length scale independent of the length of the pipe. However, the validity of definition (4) for the partially confined fluidic nozzle configuration ($2 < L/D < 3$) has yet to be adequately assessed.

Eq. (4) can be rearranged as follows:

$$\mathrm{St}_M \equiv \left(\frac{D}{d_1}\right)^2 \frac{2}{\sqrt{\pi}}\mathrm{St}_1 \tag{5}$$

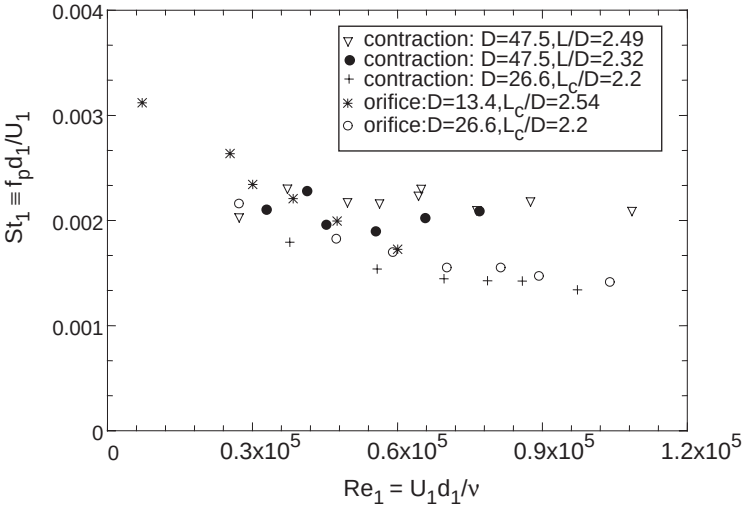

Fig. 6. Dependence of the internal precession Strouhal number St_1 on the Reynolds number Re_1.

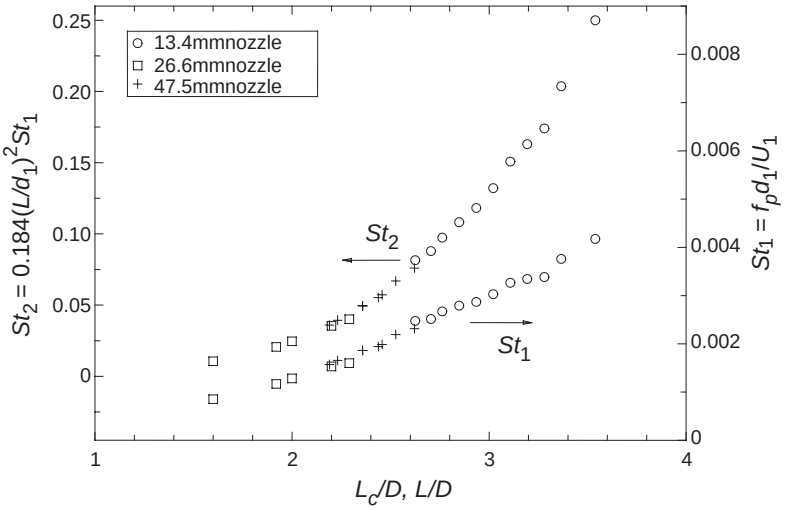

Fig. 7. Dependence of the internal and external precession Strouhal numbers St_1 and St_2 on the chamber length L^*.

since $M = \rho U_1^2(\pi d_1^2/4)$ for this case. Further substituting $D/d_1 \approx 5.1$, which applies for all the present nozzles, we obtain this $St_M \approx 29.4St_1$.

5. Reynolds and precession Strouhal numbers for external precessing jet flow

Eqs. (3) and (5) have demonstrated that the Strouhal numbers St_h, St_1 and St_M, defined by (1), (2) and (4), are related proportionally with each other by D/d_1 (the inlet expansion ratio). That is, these three numbers are essentially similar. However, only St_1 is dimensionally identical to the previous definition of Strouhal number describing the mechanically precessing jet (MPJ) from a mechanically rotating nozzle, except that different length and velocity scales are used, namely

$$St_e \equiv \frac{f_p d_e}{U_e};$$

here f_p, d_e and U_e are the nozzle rotating frequency, exit diameter and jet bulk exit velocity, respectively. In contrast, the length and velocity scales in Eqs. (1)–(5) are based on inlet parameters of the nozzle. Hence, despite the apparent similarity, the definitions for the MPJ and FPJ nozzles are significantly different and Eqs. (1)–(5) cannot be used to directly describe the flow downstream of the FPJ nozzle. Similarly, the Reynolds number previously used for the FPJ defined as $Re_1 \equiv U_1 d_1/\nu$ is also based on the jet inlet conditions and may differ from that characterising the external flow. In this context, both new Reynolds number and new precession Strouhal number for the external flow from the FPJ nozzle are sought based on the exit length and velocity scales.

We first define "external" Reynolds and Strouhal numbers based on the precession frequency (f_p), a characteristic exit jet "diameter", D_2, and axial bulk mean velocity, U_2, of the jet at the chamber exit. These lead to

$$Re_2 \equiv \frac{U_2 D_2}{\nu},$$

and

$$St_2 \equiv \frac{f_p D_2}{U_2}. \tag{6}$$

However, the complexity of the emerging flow is such that it is not possible to obtain absolute definitions of D_2 or U_2 and the detailed phase-averaged measurement is yet to be completed. The instantaneous precessing jet does not fully fill the exit plane [Nathan et al. (1998)] and there is a large amount of incoming fluid through that plane, rendering any definition of the "edge" of the outgoing jet somewhat subjective. Moreover, the emerging jet is far from circular in cross section [Wong et al. (2003)].

Given the above limitations in present understanding of the emerging flow and the complexity of the task, we apply an analytical approach to derive first-order characteristic length and velocity scales at the exit of the nozzle chamber. Recognizing that any such scales will necessarily involve arbitrary definitions, we choose to base the analysis on the well-established development of a free jet traversing an equivalent distance to the chamber length.

For a circular free jet, with initial diameter d and bulk mean velocity U_b, the jet centreline mean velocity U_c and half-radius $R_{1/2}$ (at which the local mean velocity is a half of U_c) in the flow region sufficiently downstream from the nozzle exit were found to satisfy the following relations [e.g., Hussein et al. (1994)]:

$$U_c \approx 6.0 U_b (x/d)^{-1} \tag{7}$$

and

$$R_{1/2} \approx 0.10x, \tag{8}$$

where x is the distance from the jet source or (virtual) origin. Correspondingly, the local jet diameter should be

$$D_{2f} \approx 4R_{1/2} \approx 0.40d(x/d)^1. \tag{9}$$

Previous free-jet measurements [e.g., Hussein et al. (1994)] have also indicated that, when $x/d \geqslant 10$–15, the radial profiles of the mean velocity normalized by U_c as a function $\eta = r/R_{1/2}$ becomes similar and can be well described by the Gaussian distribution $G(\eta) = \exp(-\eta^2 \ln 2)$. The local jet bulk mean velocity U_{2f} therefore can be estimated based on $G(\eta)$; that is,

$$U_{2f} = \frac{4}{\pi D_{2f}^2} \int_0^\infty 2\pi U_c R_{1/2}^2 G(\eta)\eta \, \mathrm{d}\eta \approx 0.36 U_c.$$

Substituting (7) into the above leads to

$$U_{2f} \approx 2.17 U_b (x/d)^{-1}. \tag{10}$$

Eqs. (7)–(10) hold for the free jet.

When the jet is confined in a circular chamber with diameter D, relations (7)–(10) may be modified due to the confinement; the degree of modification depends on the expansion ratio $R\,(= D/d_1)$. It is logic by dimensional analysis to replace (9) and (10) by (11) and (12) for the local diameter D_2 and bulk mean velocity U_2 of the confined jet at the chamber exit where $x = L$ (note that U_1 and d_1 is the initial bulk velocity and diameter of the jet):

$$D_2 = K_1 d(L/d_1)^m \tag{11}$$

and

$$U_2 = K_2 U_1 (L/d_1)^{-n}. \tag{12}$$

Here K_1 and K_2 are constants determined by experiments. The exponents m and n are expected to depend on the expansion ratio R; they should be equal to 1 when R is sufficiently high. Previous investigations of the confined jet [e.g. Yule and Damou (1991)] suggest that m is only slightly less than unity while $n \approx 1$. In this sense, it is not unreasonable to use the approximations $m \approx 1$ and $n \approx 1$ for estimation of D_2 and U_2. We therefore rewrite (5) and (6) as

$$\mathrm{Re}_2 = C_1 \mathrm{Re}_1 \tag{13}$$

and

$$\mathrm{St}_2 = C_2 (L/d_1)^2 \mathrm{St}_1, \tag{14}$$

where $C_1 = K_1 K_2$ and $C_2 = K_1/K_2$. Under the first-order approximation, assuming $K_1 = 0.4$ and $K_2 = 2.17$ based on the free-jet case, we obtain

$$\mathrm{Re}_2 \approx 0.87 \mathrm{Re}_1 \tag{15}$$

and

$$\mathrm{St}_2 \approx 0.184 (L/d_1)^2 \mathrm{St}_1. \tag{16}$$

Eq. (15) shows that the Reynolds number only decreases by about 13% between the chamber inlet and outlet, regardless of L, so that Re_1 is still representative of the external PJ flow. In contrast, the "external" Strouhal number St_2 is at least an order of magnitude higher than the 'internal' counterpart St_1 since normally $10 < L/d_1 < 20$. This is demonstrated in Fig. 5, which plots the measured variations of both St_1, defined by (2), and St_2, estimated from (16), against L^*. It is evident that St_1 depends approximately linearly on L^*. By comparison, St_2 is a nonlinear and strong function of L^*.

6. Effects of Re_2 and St_2 on downstream mean flow field

Using a mechanically precessing jet (MPJ), Schneider (1996) and Nobes (1998) have demonstrated that the precession Strouhal number is the primary parameter controlling the downstream development and mixing characteristics of the nonreacting MPJ flow. In comparison, the influence of jet Reynolds number, at least in the turbulent regime, is negligible. Similarly, Nathan et al. (1996) found that the Strouhal number has a controlling influence on the characteristics of a jet flame. On this basis it is reasonable to expect that the external Strouhal number of the FPJ flow will similarly exert a controlling influence on the flow and flame. However, the differences between the near-field MPJ and FPJ flows, described earlier, means that neither the dominance of St nor a direct correlation in terms of their effect on the downstream mixing or reaction, can be assumed a priori. More insight into these issues can be obtained by comparing St_2 defined above, with St_e for the MPJ nozzle.

Fig. 8 shows the axial variations of the total mean pressure (p_t) measured on the nozzle axis in the external flow relative to its value at $x_2/D = 0$, i.e., $p_t(x_2)/p_t(0)$, where x_2 is measured from the chamber exit. The results were obtained with a FPJ nozzle whose chamber diameter D= 26 mm and chamber inlet diameter $d_1 = 5.2$ mm. This nozzle also used a centre-body (inside the chamber) with a diameter of $d_c = 19$ mm. In one case the chamber length was varied to change the frequency, in another the flow-rate was varied to change the Reynolds number. The three cases tested can thus be specified as: (a) $Re_2 \approx 26{,}000$ and $L_c/D = 2.3$; (b) $Re_2 \approx 64{,}000$ and $L_c/D = 2.3$; and (c) $Re_2 \approx 64{,}000$ and $L_c/D = 1.6$. The external precession Strouhal number St_2, estimated from Eq. (16), is about the same, i.e. $St_2 \approx 0.04$, for cases (a) and (b), while $St_2 \approx 0.01$ for case (c).

It is evident from Fig. 8 that the normalized total mean pressure along the nozzle axis is quite similar for cases (a) and (b), suggesting a broader similarity in their external flows for different values of Re_2. In other words, as for the MPJ counterpart, variations in Reynolds number within this fully turbulent regime do not appear to have a significant effect on the mixing field of the FPJ flow. In contrast, the impact of variation in the precession Strouhal number made by changing the chamber length appears to be very significant. Substantial differences in the external total pressure field are evident for cases (b) and (c) where $St_2 = 0.04$ and $St_2 = 0.01$, respectively. The total mean pressure peaks at a greater downstream distance for the higher Strouhal number than the lower one.

The results presented in Fig. 8 should not be considered to be quantitative due to the fact that the emerging flow has large fluctuations in direction and time. Although the frequency response of the total pressure probe (> 500 Hz) is much higher than the dominant frequency of precession (30–80 Hz), the flow is not always well aligned to the probe. Nevertheless, while the absolute accuracy of the p_t measurements is limited, the relative accuracy is sufficient to demonstrate strong dependence of the downstream FPJ flow on St_2 and weaker dependence on Re_2.

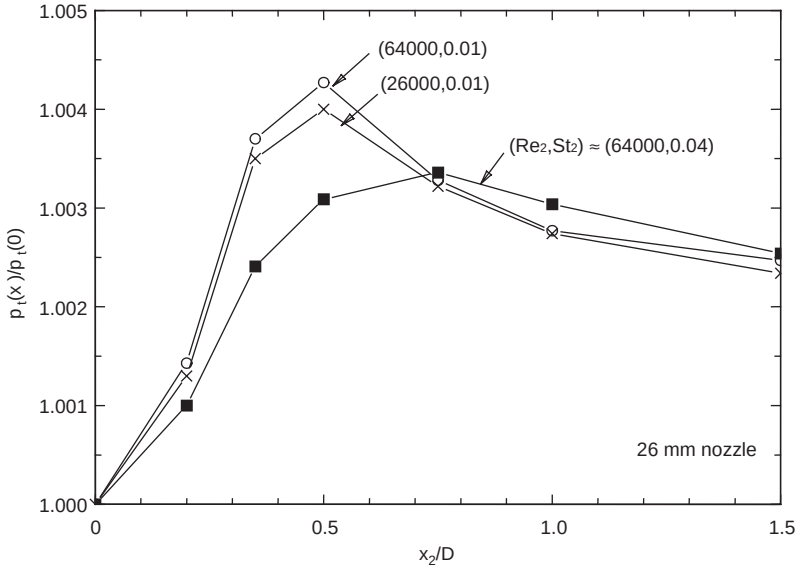

Fig. 8. Axial variations of the mean total pressure along the nozzle axis: ○, $Re_2 \approx 64000$ and $St_2 \approx 0.04$; ■, 26000 and 0.04; ×, 64000 and 0.01.

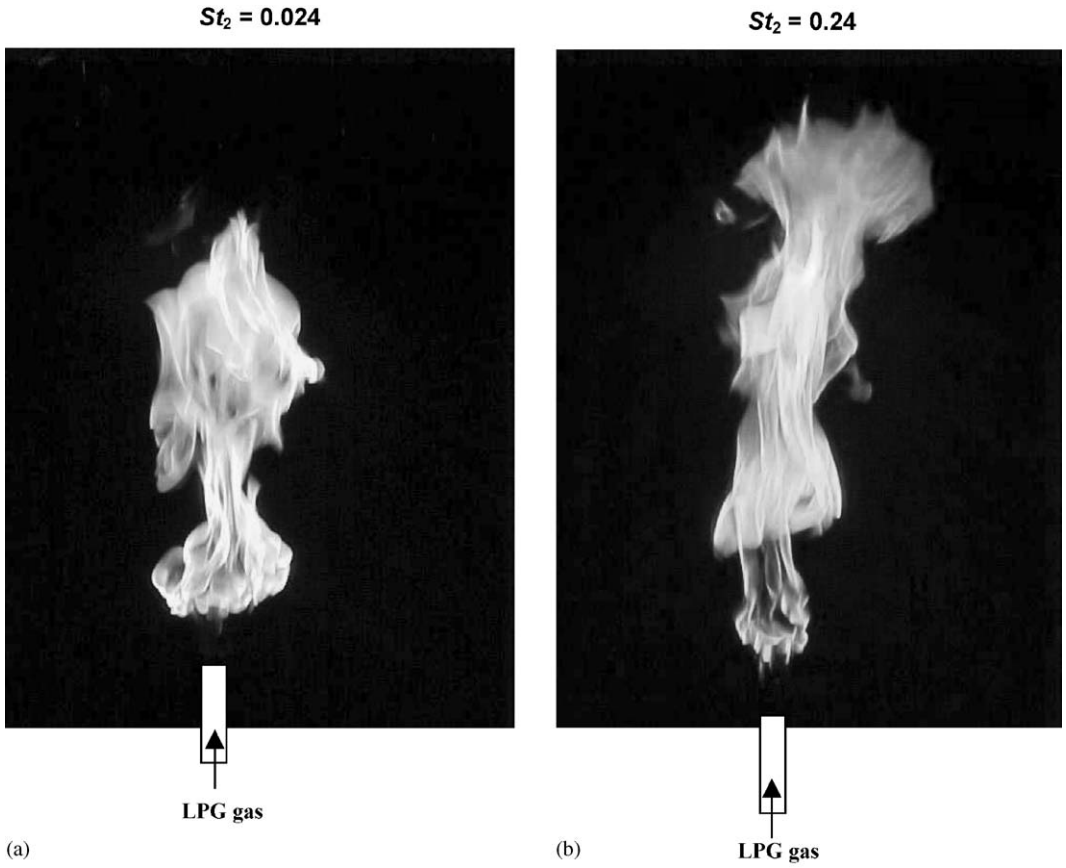

Fig. 9. Effect of the external precession Strouhal number St_2 on the PJ flame at $Re_1 \approx 32{,}000$: (a) $St_2 = 0.024$; (b) $St_2 = 0.24$.

It should be noted however that the above conclusion is deduced only from the first-order mean pressure data, not from higher-order pressure fluctuations, and therefore may not apply for those higher-order quantities such as Reynolds stresses. In other words, the turbulent fluctuating field could still depend on the Reynolds number even though the mean field does not.

To further assess the impact of St_2, two typical instantaneous images of the FPJ flame are presented in Fig. 9 for $St_2 \approx 0.024$ and 0.24, respectively. A smaller (brass) nozzle was used, with $D = 13.4$ mm, to limit the size of the flame. The values of $St_2 \approx 0.024$ and 0.24 were obtained with the chamber length of $L_c/D \approx 2$ and 3.5. Several observations can be made. The flames for both Strouhal numbers are luminous. However, the flame for $St_2 \approx 0.024$ is shorter but more bulbous than that at $St_2 \approx 0.24$. The flames also show clear evidence of the presence of large-scale dominant structures (two for $St_2 \approx 0.024$ and three to four for $St_2 \approx 0.24$) identified by Newbold et al. (1997) which is characteristic of high Strouhal number flames. At this point, it is useful to compare the magnitudes of St_1 and St_2 determined for the present FPJ flames with the value of St_{cr} determined previously for the MPJ flames. The magnitude of St_1 for the present flames are 0.0025 and 0.004, respectively, which are both far below that of the critical Strouhal number $St_{cr} \approx 0.03$ found by Nathan et al. (1996) for the MPJ flame. Since the flames are evidently in the super-critical regime, this confirms the earlier deduction that St_1 is not representative of the external flow. Comparison of the lower value of $St_2 = 0.024$ with the MPJ $St_{cr} = 0.03$ suggests that, while being more appropriate than St_1, it may still under-estimate the true value of the external Strouhal number. This is somewhat consistent with the finding of Wong et al. (2003) that the jet within the chamber decays more rapidly than a free jet, which would result in the true exit "diameter" being larger, and the true exit velocity being lower, than those derived for St_2 based on the free-jet mean velocity field.

7. Final remarks

The effects of the nozzle chamber length (L) and the jet inlet velocity (U_1) on the jet precession frequency (f_p) have been examined. It has been shown that f_p increases approximately linearly with U_1 for the present range of conditions in which the flow is turbulent and incompressible. The frequency also increases approximately linearly with L over the range $1.6 < L/D < 3.6$ where the precession occurs continuously. Since previous definitions of precession Strouhal number, Eqs. (1) and (4), do not account for the L effect, they likewise show the same L dependence as the precession frequency (Fig. 7). These Strouhal numbers, however, are inappropriate for characterizing the turbulent mixing downstream from the chamber exit because they are all based on the chamber inlet conditions.

A correlation-based approach has been applied to advance understanding of the relationship between the internal and external Strouhal numbers for the FPJ nozzle. The empirical values for the circular free jet were used in the absence of better information of the instantaneous emerging PJ flow. This has resulted in a new definition of external Strouhal number

$$\mathrm{St}_2 = C_2(L/d_1)^2\mathrm{St}_1,$$

where $C_2 \approx 0.184$ is the corresponding value based on the constants for the circular free jet. Since the actual jet in the chamber spreads and decays at different rates from the free jet, the true value of C_2 is likely to be somewhat different. Measurements of the mean total pressure obtained along the FPJ nozzle axis in the downstream flow for three different conditions have shown that St_2 has a significant influence on the oscillating mixing field, while Reynolds number does not. This trend is consistent with previous measurements on the MPJ flow.

The characters of the flames from the 13.4 mm nozzle appear to be similar to those of the super-critical MPJ flames in which the magnitude of the external Strouhal number exceeds the critical value $\mathrm{St}_{cr} = 0.03$ (Nathan et al., 1996). The smaller value of St_2 as obtained using $C_2 = 0.184$ derived from the free jet is 0.024, although the observation from the corresponding flame (Fig. 7) suggests it to be supercritical. This implies that the C_2 value derived from the free jet results in an under-estimate of the true external Strouhal number. To enable the FPJ flame characteristics to be consistent with those of the MPJ, we suggest that $C_2 = 0.25$ is representative. On this basis, the external precession Strouhal number can be characterized usefully by

$$\mathrm{St}_2 = 0.25(L/d_1)^2\mathrm{St}_1.$$

Acknowledgements

The collaborative support of the Australian Research Council and Fuel & Combustion Technology Ltd is gratefully acknowledged.

References

Hill, S.J., Nathan, G.J., Luxton, R.E., 1995. Precession in axisymmetric confined jets. In: Bilger, R.W. (Ed.), Proceedings of 12th Australiasian Fluid Mechanics Conference, Sydney, pp. 135–138.

Hussein, H.J., Capp, S.P., George, W.K., 1994. Velocity measurements in a high Reynolds number, momentum-conserving axisymmetric turbulent jet. Journal of Fluid Mechanics 258, 31–60.

Luxton, R.E., Nathan, G.J., 1987. Mixing fluids. International Patent Application No. PCT/AU88/0014, Australian Patent Office (Priority date: April 1987).

Manias, C.G., Nathan, G.J., 1993. The precessing jet gas burner—a low NO_x burner providing process efficiency and product quality improvements. World Cement, March, 4–11.

Manias, C.G., Nathan, G.J., 1994. Low NO_x clinker production. World Cement, May 25(5), 54–56.

Manias, C.G., Nathan, G.J., Rapson, D.S., 1995. Gyro-Therm: a new efficient low NO_x gas burner for product quality improvement. ASEAN Federation of Cement Manufacturers, Kuala Lumpur.

Mi, J., 1996. Frequency characteristics of various oscillating jets. Research Report, Department of Mechanical Engineering, University of Adelaide, Australia.

Mi, J., Nathan, G.J., 2000. Precession Strouhal number of a self-excited precessing jet. In: Proceedings of Symposium on Energy Engineering in the 21st Century, Hong Kong, pp. 1609–1614.

Mi, J., Nathan, G.J., Luxton, R.E., 1997. Frequency spectra of turbulence in a precessing jet. In: Proceedings of Seventh Asian Congress of Fluid Mechanics, Chennai, pp. 437–440.

Mi, J., Luxton, R.E., Nathan, G.J., 1998. The mean velocity field of a precessing jet. In: Proceedings of 13th Australasian Fluid Mechanics Conference, Melbourne, pp. 623–626.

Mi, J., Nathan, G.J., Hill, S.J., 1999. Frequency characteristics of a self-excited precessing jet nozzle. In: Proceedings of Eighth Asian Congress of Fluid Mechanics, Shenzhen, pp. 755–758.

Nathan, G.J., Luxton, R.E., 1991. Mixing enhancement by a self-exciting, asymmetric precessing flow-field. In: Proceedings of Fourth International Symposium on Transport Phenomena, Sydney.

Nathan, G.J., Turns, S.R., Bandaru, R.V., 1996. The influence of jet precession on NO_x emissions and radiation from turbulent flames. Combustion Science & Technology 112, 211–230.

Nathan, G.J., Hill, S.J., Luxton, R.E., 1998. An axisymmetric 'fluidic' nozzle to generate jet precession. Journal of Fluid Mechanics 370, 347–380.

Nathan, G.J., 1988. The enhanced mixing burner. Ph.D. Thesis, Department of Mechanical Engineering, University of Adelaide, Australia.

Newbold, G.J.R., Nathan, G.J., Luxton, R.E., 1997. The large scale dynamic behaviour of an unconfined precessing jet flame. Combustion Science and Technology 126, 71–95.

Newbold, G.J.R., Nathan, G.J., Nobes, D.S., Turns, S.R., 2000. Measurement and prediction of NO_x emissions from unconfined propane flames from turbulent-jet, bluff-body, swirl and precessing jet burners. In: Proceedings of the Combustion Institute 28, pp. 481–487.

Nobes, D.S., 1997. The generation of large-scale structures by jet precession. Ph.D. Thesis, Department of Mechanical Engineering, University of Adelaide, Australia.

Schneider, G.M., 1996. Structures and turbulence characteristics in a precessing jet flow. Ph.D. Thesis, Department of Mechanical Engineering, University of Adelaide, Australia.

Schneider, G.M., Nathan, G.J., Luxton, R.E., Hooper, J.D., Musgrove, A.R., 1997a. Velocity and Reynolds stresses in a precessing jet flow. Experiments in Fluids 22, 489–495.

Wong, C.Y., Lanspeary, P.V., Nathan, G.J., Kelso, R.M., O'Doherty, T., 2003. Phase-averaged velocity in a fluidic precessing jet nozzle and in its near external field. Journal of Experimental Fluid and Thermal Science 27, 515–524.

Yule, A.J., Damou, M., 1991. Investigations of ducted jets. Experimental Thermal and Fluid Science 4, 469–490.